Energy 36 (2011) 6146–6155

Contents lists available at ScienceDirect

Energy

journal homepage: www.elsevier.com/locate/energy

Influence of direct reduced iron on the energy balance of the electric arc furnace in steel industry

Marcus Kirschen [a,b,*], Karim Badr [b], Herbert Pfeifer [a]

[a] RWTH Aachen University, Institute for Industrial Furnaces, Aachen, Germany
[b] RHI AG, Process Technology and Systems Solutions, Vienna, Austria

ARTICLE INFO

Article history:
Received 16 December 2010
Received in revised form
25 July 2011
Accepted 31 July 2011
Available online 27 August 2011

Keywords:
Energy balance
Electric arc furnaces
Direct reduced iron
Process model

ABSTRACT

A model of the EAF energy efficiency was developed based on a closed mass and energy balance of the EAF melting process. This model was applied to industrial EAFs in steel industry charged with scrap or with mixes of scrap and DRI. Complex mass and energy conversion in the EAF was simplified with the introduction of mass and energy conversion efficiencies for the conversion of oxygen and the energy conversion of electrical energy in the electric arcs, chemical energy from the oxidation reactions in the melt and energy from the combustion of burner gas. It turned out that close agreement with observed process parameters from 16 EAFs is obtained by slight variations of the efficiency values. Especially the sensitivity of the steel temperature from the energy conversion efficiency of the electric arc energy indicates the importance of efficient foaming slag operation in EAF steel making. Characteristics and process parameters of DRI charged EAFs are discussed. Model results for a series of case studies illustrate the correlations between DRI chemical composition, DRI portion, oxygen consumption, etc. with electrical energy demand in order to indentify cost-effective EAF process conditions.

1. Introduction

1413 Mio tonnes steel was produced world-wide in 2010, where 29% were produced by melting steel scrap, scrap alternatives and additives in the electric arc furnace (EAF) or rarely in the open hearth furnace [43]. 71 % of total steel production was produced by reducing iron ore with coke and coal in the blast furnace (BF) and subsequent decarburization in the basic oxygen furnace (BOF).

An alternative production route of steel is based on the reduction of iron ore to direct reduced iron, DRI, with reformed gas enriched in carbon monoxide, CO, and hydrogen, H_2. Reformer gas is produced from natural gas, biomass or gasified coal. 71.3 Mio tonnes DRI were produced in 2010 with continuously increasing trend during the last three decades despite increasing energy costs of the main reducing agent used, natural gas (Fig. 1) [43]. In 2009, 39.7% was produced in India, the world largest DRI producer, 30.2% was produced in reduction plants in Middle East and North African countries, 19.6% was produced in Latin America [30]. Main production routes are the Midrex™ process and the Hyl™ process based on natural gas (in total 73.1%). Coal-based processes comprise reduction in rotary kilns (e.g. SL/RN™), and to a much smaller amount in fluidized bed furnaces (26.9%). In 2009, 54 production plants were operational, 52 plants produced direct reduced iron [30]. DRI as raw material for steelmaking is used entirely in EAF steel plants where it is melted with or without scrap in the EAF.

Direct reduction of iron ore by charcoal to sponge iron was the very initial route of iron making. Due to the high porosity of direct reduced iron, the raw material consisted of few % slag component, but was low in carbon. The sponge iron had to be heavily forged in order to force out the slag. Hot briquetted iron (HBI) of modern reduction plants is a mechanically compacted form of DRI with lower reactivity, higher density and thermal conductivity and, consequently, better handling for packaging and more secure transport.

For the production of high quality speciality steel grades from scrap with varying quality and chemical composition, the compliance with high purity levels is sometimes only achieved with dilution of unwanted tramp elements as Pb, Cu, Cr, Ni, Mo, and Sn with highly pure substituting materials direct reduced iron and hot metal. For example, high quality tyre cord with Cu lower than 0.05% is economically produced by melting mixes of steel scrap and 50–100% DRI [14]. Due to increasing scrap prices world-wide and at regions with restricted availability of high quality steel scrap, the combination of low quality scrap grades and highly pure scrap substituting materials is a cost-effective option [14,15]. DRI is also

* Corresponding author.
E-mail address: marcus.kirschen@rhi-ag.com (M. Kirschen).

0360-5442/$ – see front matter © 2011 Elsevier Ltd. All rights reserved.
doi:10.1016/j.energy.2011.07.050

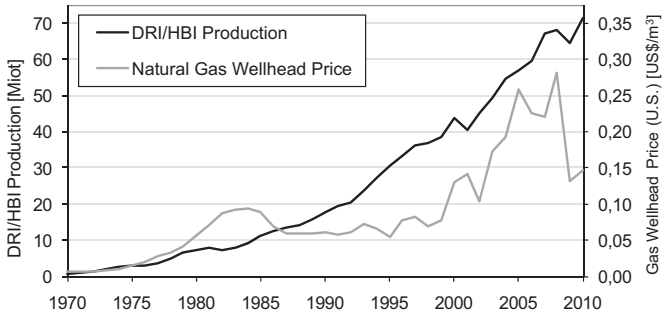

Fig. 1. Production increase of direct reduced iron world-wide versus natural gas wellhead price U.S. ([41,43] and U.S. energy agency).

used for economic high quality steel production with low nitrogen and very low phosphorus and hydrogen content [14,16,26]. The nitrogen content of tapped steel in the EAF decreases from 40 to 100 ppm N_2 for 100% steel scrap charges to 15–25 ppm for DRI charges [4,28]. Low nitrogen limits of the steel products require extensive Ar purging and/or vacuum degassing.

1.1. DRI production routes

The demand for direct reduced iron increased dramatically during the last two decades (Fig. 1). Reducing agents of iron ore fines are reformer gas from natural gas, coal or gasified coal.

The chemical and physical properties of direct reduced iron and hot briquetted iron are rather varying due to the different reduction routes, e.g. gas-based reduction of pellets and lump ore (e.g. Midrex™, Hyl™), gas-based reduction of fine ore (e.g. Fior™, Finmet™, Circored™, Circofer™), coal-based fluidized bed reduction processes (e.g. Finex™, Fastmet™) and rotary kiln based processes (e.g. SL/RN™), and due to the used ore grades, ore blends, gangue materials, metallization grades, and additives [14,15]. The compaction of direct reduced iron to HBI is applied to fluid-bed processes for fine ore (e.g. Finmet™, Circored™, Fior™) and shaft furnace processes for pellets and lump ore (Midrex™, Hyl™).

The principal reduction reactions converting hematite iron ore with reformer gas to DRI are:

$$Fe_2O_3 + 3CO = 3CO_2 + 2Fe \quad (1)$$

$$Fe_2O_3 + 3H_2 = 3H_2O + 2Fe \quad (2)$$

Natural gas-based DRI production is more widely produced with respect to the coal-based process and it is characterised with higher metallization and carbon (Table 1).

A low degree of metallization means more FeO has to be reduced in the EAF. On the other hand, a high metallization degree results in less CO generation and lower bath agitation in the EAF, which in turn reduces the heat transfer efficiency and accordingly increases the furnaces energy requirements [14–16]. The best results are obtained when metallization of DRI lies between 94% and 96%. Common metallization is close to 94% [9,10,25].

Table 1
Properties and chemical compositions of direct reduced iron [7,15,28,31].

	Degree of metallization	Fe_{total}	Fe_{metal}	Carbon content %	Gangue material	
					Acid %	Basic %
NG based	92–96	91–93	84–88	1.0–2.5	2.5–5.0	0.5–2.7
Coal based	92–93	90.4–93.7	83–87	0.1–0.2	3.2–7.6	0.1–0.35

DRI has high bulk density, which is greater than that of most types of steel scrap. Its density is higher than that of the slag in the furnace, which facilitates its melting at the slag/metal interface. The remaining FeO in the DRI reacts with the carbon in the liquid metal bath to improve the foaming slag that shields the refractory from the arcs. However, DRI feeding rate is an important parameter of the EAF process that has to be controlled. The optimum feeding rate depends on the DRI chemical composition, the bath temperature, and the stirring energy provided by the oxygen carbon injectors and the bottom stirring plugs. DRI feeding rates of most DRI furnaces are in the range between 27 and 35 kg/min MW.

Looking at the role of carbon in the DRI, it should be noted that about two-thirds of the carbon contained in DRI is present as iron carbide, Fe_3C, and the balance is deposited as free carbon. The reactions involved in carburizing the DRI, for iron carbide production are:

$$3Fe + CH_4 = Fe_3C + 2H_2 \quad (3)$$

$$3Fe + CO + H_2 = Fe\left(C_{free}\right) + H_2O \quad (4)$$

It should be noted that the carbon produced in DRI (NG based) is usually more than the stoichiometric requirements needed to reduce the remaining portion of FeO in the product. DRI contains about 11 kg_C/t_{DRI}. The excess carbon has significant impact on the FeO content of the slag and on the slag foaming that is required for an efficient EAF melting process [37]. In case of negative excess carbon, the necessary addition of coal for FeO reduction is beneficial when late in the EAF process [32,37]. However, not all the iron oxide is reduced into Fe since a portion of the FeO does always exist in the furnace slag. This means that the practical amount of excess carbon of DRI that is available for combustion in the steel bath, is more than the excess carbon calculated for DRI reduction. This term is called combustible carbon and defined as:

$$x_{\text{Combustible Carbon}} = x_{C,DRI} - x_{C,\text{stoichiometric}}\left(x_{FeO,DRI} - x_{FeO,Slag}\right)$$

The combustible carbon reacts with the oxygen injected to the melt in the EAF, to release heat in the steel bath and also contribute CO gas in the slag foaming. With increasing combustible carbon in the EAF the nitrogen content of the tapped steel decreases [28]. Excess carbon from the DRI decreases the input of anthracite or injected graphite fines that is a major source for dissolved N in the EAF (0.1% N_2) besides infiltrated air [28]. A second benefit obtained from the carbon in DRI is through the energetic benefits of Fe_3C. Fe_3C yields energy through the exothermic reactions obtained during its dissociation in the steel bath, −0.4 kWh/kg_C [18], in contrast to endothermic dissolution of carbon particles in the steel bath, 0.62 kWh/kg_C [18].

1.2. CO_2 emission figures

All studies of specific CO_2 emission of different steelmaking routes show a lower emission figure for EAF steelmaking based on melting of steel scrap with mainly electrical energy versus reduction of iron ore with coke in the blast furnace. Detailed calculations of recent energy intensities and CO_2 emission figures in the steel industry have been published, e.g. [3,5,8,11,12,15,16,18,24,29,35,37,44,46].

Due to the hydrogen content as ferrous iron reducing agent, the CO_2 emission figure of the DRI-EAF production route is smaller than for the blast furnace production route. However, DRI production sites are mainly restricted to areas with high availability of natural gas and the restricted availability of high quality scrap. Indirect CO_2

emission from generation and provision of electricity has to be taken into account for the EAF steel production introducing an additional variation in CO_2 emission figure of DRI-based steelmaking process. Specific electrical energy demand of DRI melting in the EAF is higher than steel scrap melting with values in the range 310–640 kWh/t_{Steel} due to lower metal yield, additional gangue material resulting in higher specific slag mass and endothermic reduction reaction of FeO and excess carbon in DRI melts. CO_2 intensity of electricity ranges from, e.g. 0.081 $kgCO_2$/kWh (Brazil) to 0.788 $kgCO_2$/kWh (China) [13].

Current total carbon dioxide emissions of the BF-BOF based steel production are reported in the range 1630–1960 kg_{CO2}/t_{Steel}, 360–470 kg_{CO2}/t_{Steel} for the scrap-based raw steel production in the EAF, and 560–1450 kg_{CO2}/t_{Steel} for DRI-based raw steel production in the EAF (Table 2).

Based on a detailed thermodynamic analysis of FeO_x reduction process by carbon in the BF Scholz [38] determined the minimum value of CO_2 emission to 1371 kg_{CO2}/t_{Steel} (theoretical minimum due to chemical restrictions) and 1518 kg_{CO2}/t_{Steel} (technical minimum due to non-zero mass and energy conversion losses). A recent benchmark of BF processes in Europe pointed the best 10% benchmark to 1475 kg_{CO2}/t_{Steel} with an industry average of 1630 kg_{CO2}/t_{Steel} indicating that current BAT technology for BF in Europe approached minimum emission level [29]. Minimum emission values determined by Fruehan et al. [12] for the BF process, 1091–1158 kg_{CO2}/t_{Steel}, are however lower because conversion losses were neglected.

The range of emission values of the DRI-based EAF steel production is spread due to varying DRI to scrap ratio in the EAF an due to different DRI production processes. E.g., typical emissions of gas-based reduction of lump ore and pellets (Midrex process) is in the order of 556 kg_{CO2}/t_{DRI} whereas the gas-based reduction of ore fines in a Finmet plant emits 771 kg_{CO2}/t_{DRI} [33]. The overall emission of the DRI production including electricity emissions is in the order of 904 kg_{CO2}/t_{DRI} (Midrex) and 993 kg_{CO2}/t_{DRI} (Finmet), respectively [33].

A case study for DRI-based EAF steel production in South Africa (with 0.869 kg_{CO2}/kWh_{el} electricity emissions [13]) resulted in total specific CO_2 emissions of steelmaking via melting of DRI in the EAF of 1240 kg_{CO2}/t_{Steel} (Midrex) to 1302 kg_{CO2}/t_{Steel} (Finmet) [33]. The total emission figure is more advantageous for countries with low specific CO_2 emission of electricity generation, e.g. for Venezuela (0.208 kg_{CO2}/kWh_{el} [13]): 866 kg_{CO2}/t_{Steel} (Midrex) and 943 $kgCO_2/t_{Steel}$ (Finmet) versus 1712 kg_{CO2}/t_{Steel} for a modern BF-based steel production [33].

CO_2 emission figures by carbon mass balances of EAF based steelmaking processes are given in Table 2 and Fig. 2 including the emissions from electricity generation. Process related carbon dioxide emissions of the EAF process comprise the initial carbon content of DRI, coal addition and carbon fines injection for slag foaming, and natural gas burners. Recent carbon mass balances of industrial EAF processes in Germany with 100% scrap charges showed values in the range from 20 kg_C/t_{Steel} to 55 kg_C/t_{Steel}, i.e. direct CO_2 emissions from 70 to 200 kg_{CO2}/t_{Steel} in agreement with an independent benchmark from a plant supplier [36].

Table 2
Reported total CO_2 emissions of different routes of steelmaking in kg_{CO2}/t.

BF with coke, sinter	BOF	EAF, DRI based	EAF, scrap based	Reference
1950		1316		[3]
1922		1310–1452		[5]
1695		984–1147		[6]
1750		870	360	[8]
1850		1090		[11]
1447–1559	189–207		364–416	[12]
1091[a]–1158[b]			225[a]–277[b]	[12]
		632–1880	441	[15]
1922–1959		912–1259	441	[16]
1959		713–1140	466	[24]
1371[a]–1518[b]				[38]
1696	148			[46]

[a] Theoretical minimum value excluding electricity.
[b] Practical minimum value excluding electricity.

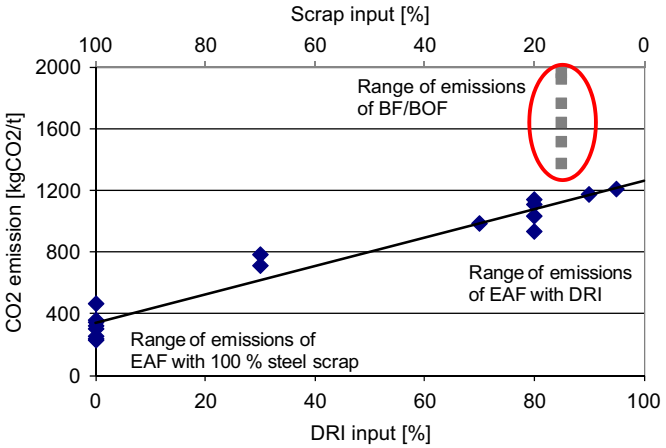

Fig. 2. Specific CO_2 emission from process data including the contribution from electricity generation [13] as function of DRI to scrap ratio for steel production routes in EAF (charged with scrap and DRI, 565 kg_{CO2}/t_{DRI}) and BF/BOF (approx. 15% scrap).

The direct reduction of iron ore below the iron melting point is therefore characterized by significant energy savings compared to the blast furnace route. Due to the use of natural gas or gasified coal the CO_2 emission figure of DRI plants is also lower when compared to the blast furnace. Parts of the carbon used for iron ore reduction are replaced by hydrogen of the process gas of converted natural gas or gasified coal.

Most DRI production plants are located near production sites of natural gas with minimum transport costs, e.g. Iran, India, Venezuela [30].

2. Determination of the complete and the dynamic energy balance

EAF energy sources comprise electrical energy and energy generated from oxidation reactions during refining (Fig. 3, Eq. (1)). Natural gas burners and carbon-oxygen injectors are used to increase energy intensity in the EAF, to avoid cold spots in eccentric furnace designs, to accelerate the scrap melting time, and to increase productivity in the case of restricted transformer power. When the energy balance boundary encompasses only the EAF

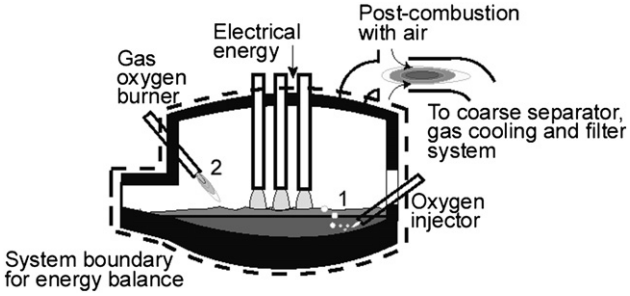

Fig. 3. Electrical energy and chemical energy sources comprising gas burners and oxidation reactions from oxygen injection in the EAF.

vessel (Fig. 3) any additional energy input, for example from scrap pre-heating systems, must be accounted for separately as well as the additional energy contributions from the input of hot metal and hot direct reduced iron.

Precisely determining the total energy input into an EAF is complex because energy is supplied to the EAF from multiple sources: Electrical energy as well as chemical energy that is released from the combustion of NG, liquefied petroleum gas or oil, and due to the oxidation of elements in the melt during refining, for example C, Si, Al, Fe, Cr, and Mn (Fig. 4). The latter energy contribution is not only dependent on the oxygen input but also on the chemical composition of the raw steel melt and slag. The electrical energy requirements of EAF steel plants are in the range of 350–550 kWh/t. Decreasing the mean electrical energy requirement and decreasing the mean specific NG consumption (i.e. 21 m^3/t in 1991 to 10 m^3/t in 2008) correlated with an increased specific oxygen consumption (i.e. 24 m^3/t to 35 m^3/t, respectively) [18].

2.1. Closed energy balances

In this paper energy balances are examined for EAF processes charged with 100% steel scrap up to 100% DRI. For this purpose we set-up an energy model to determine the process parameters as weight, composition and temperature of the steel melt at tap, slag weight and composition as functions of input parameters weight and composition of steel scrap, DRI, and other ferrous input, slag formers, energy input, etc.

The total EAF energy balance is given by Eq. (5):

$$E_{\text{Total}} = E_{\text{In}} = \int_{\text{Charging}}^{\text{Tapping}} P_{\text{Electric}}\,dt + \Delta H_{\text{Oxygen Injection}} + \Delta H_{\text{NG burners}}$$
$$= E_{\text{Out}} = \Delta H_{\text{Steel}} + \Delta H_{\text{Slag}} + \int \Delta \dot{H}_{\text{Off-gas}}\,dt + \int \Delta \dot{Q}_{\text{Cooling}}\,dt + \int \Delta \dot{Q}_{\text{Radiation, other losses}}\,dt \quad (5)$$

The steel and slag enthalpies are dependent on the tapped masses and specific enthalpies, namely the actual chemical compositions. Heat losses from the system are due to water-cooling of the furnace vessel, roof, and hot gas duct as well as radiation losses to the surroundings during charging and lining repair when the EAF roof is open. Ohmic losses from the high current system between the transformer and electric arc account for 6–10%. The chemical energy input is the sum of the reaction enthalpies (Eq. (6)) due to metal (Me) oxidation (e.g. C, Si, Mn, Al, P, Cr, Ni, and Fe):

$$\Delta H_{\text{Oxygen Injection}} = \sum_{\text{Me}} m_{\text{Me}} \Delta h_{\text{Me}} \quad (6)$$

Δh_{Me} is the specific reaction enthalpy of Me oxidation. The specific reaction enthalpies range from 1.32 kWh/kg_{Fe} for FeO, 2.55 kWh/kg_C for CO, to 8.94 kWh/kg_{Si} for SiO_2 (Table 3). Energy and CO_2 emission levels resulting from the combustion of different NG grades with oxygen, $\Delta H_{\text{NG burner}} = h_u V_G$, are in the range 9.3–10.7 kWh/m^3 depending on chemical composition of the natural gas.

Additional energy terms comprise the endothermic solution enthalpy of carbon in the steel melt, −0.62 kWh/kgC. This is important if carbon is charged as coke or coal to the furnace and has to be dissolved in the steel melt before oxidation whereas the solution enthalpy of carbon is not considered when iron with a defined carbon content as pig iron (3.5% C from production in a cupola furnace, 4.1–4.4% C by reduction with coal or coke), direct reduced iron (0.1–4% C depending on production details) or hot metal (4.2% C) is charged to the EAF. The enthalpy that is released from the oxidation of carbon has to be decreased with the enthalpy of carbon dissolution if carbon is charged as coke or coal to the EAF. This contributes to the energetic advantage of using carbon containing raw materials as DRI, pig iron or hot metal in the EAF.

The more important endothermic energy sink in the EAF is due to the reduction of FeO in slag by C: FeO + C = Fe + CO releasing −3.59 kWh/kgC energy. The endothermic reduction reaction FeO + C = Fe + CO has to be considered for the internal reduction of DRI or HBI and for the reduction of FeO component in the slag when carbon is injected to generate foaming slag by CO gas production in the slag layer.

The total energy intensities in the EAFs examined ranged from 650 kWh/t to 850 kWh/t (Fig. 4). An increased energy efficiency requires decreased energy losses to the EAF off-gas and water-cooling systems. The large variation in energy losses to these sinks indicates a high potential for energy savings. The CO_2 emission intensities of EAFs (m_{CO2}/E_{Total}) are in the order of 0.15 kg_{CO2}/kWh [44]. Recently measured CO_2 intensities from EAFs in Germany ranged from 0.11 to 0.21 kg_{CO2}/kWh [18].

In order to provide a time dependent energy balance of the EAF, we derived the energy content of the EAF at a distinct time of melting as time derivative of Eq. (5) (Eq. (7)).

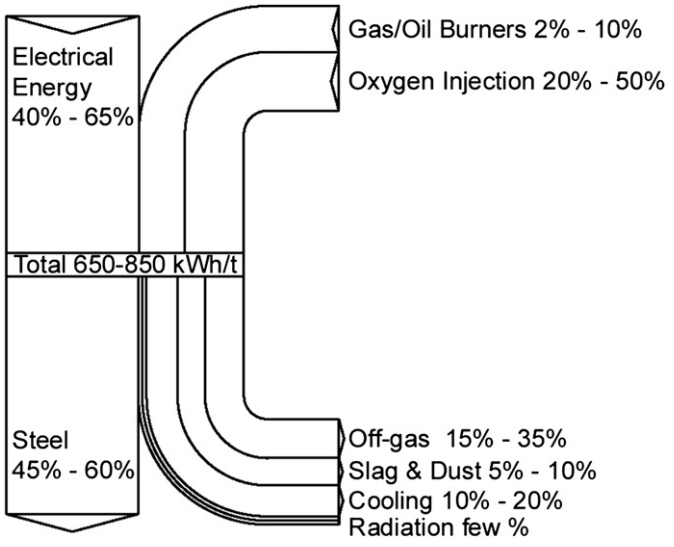

Fig. 4. Energy sources in an EAF (e.g. electrical energy and chemical energy resulting from oxidation reactions) and energy sinks (e.g. off-gas extraction and furnace cooling systems).

Table 3
Exothermic oxidation reactions and energy released during steel melt refining [18].

	Energy released	
Reactions in melt		
$Si + O_2 \rightarrow SiO_2$	8.94 kWh/kg_{Si}	11.2 kWh/$m^3_{O_2}$
$Mn + 0.5O_2 \rightarrow MnO$	1.93 kWh/kg_{Mn}	9.48 kWh/$m^3_{O_2}$
$2Cr + 1.5O_2 \rightarrow Cr_2O_3$	3.05 kWh/kg_{Cr}	9.42 kWh/$m^3_{O_2}$
$2Fe + 1.5O_2 \rightarrow Fe_2O_3$	2.05 kWh/kg_{Fe}	6.80 kWh/$m^3_{O_2}$
$Fe + 0.5O_2 \rightarrow FeO$	1.32 kWh/kg_{Fe}	6.58 kWh/$m^3_{O_2}$
$C + 0.5O_2 \rightarrow CO$	2.55 kWh/kg_C	2.73 kWh/$m^3_{O_2}$
$2Al + 1.5O_2 \rightarrow Al_2O_3$	5.29 kWh/kg_{Al}	13.84 kWh/$m^3_{O_2}$
$Mo + O_2 \rightarrow MoO_2$	1.70 kWh/kg_{Mo}	7.29 kWh/$m^3_{O_2}$
$S + O_2 \rightarrow SO_2$	2.75 kWh/kg_S	3.94 kWh/$m^3_{O_2}$
$2P + 2.5O_2 \rightarrow P_2O_5$	5.54 kWh/kg_P	8.58 kWh/$m^3_{O_2}$
Reactions in gas phase		
$C + O_2 \rightarrow CO_2$	9.10 kWh/kg_C	4.88 kWh/$m^3_{O_2}$
$CO + 0.5O_2 \rightarrow CO_2$		7.01 kWh/$m^3_{O_2}$
$H_2 + 0.5O_2 \rightarrow H_2O$		5.99 kWh/$m^3_{O_2}$

The enthalpy that is heating up the melt and slag in a small time step Δt is determined from the energy input from the electric arcs (P_{Electric}), from oxidation reactions, and from the gas burners ($P_{\text{NG Burners}}$).

$$\begin{aligned}\Delta E_{\text{Total}} &= \int_{t}^{t+\Delta t} P_{\text{Electric}}\,dt + \int_{t}^{t+\Delta t} \sum_i \dot{m}_{\text{Oxidized,i}} h_{\text{Oxidized,i}}\,dt \\ &\quad + \int_{t}^{t+\Delta t} P_{\text{NG Burners}}\,dt \\ &= \int_{T(t)}^{T(t+\Delta t)} h_{\text{Steel}} m_{\text{Steel}}\,dt + \int_{T(t)}^{T(t+\Delta t)} h_{\text{Slag}} m_{\text{Slag}}\,dt \\ &\quad + \int_{t}^{t+\Delta t} P_{\text{Off-gas}}\,dt + \int_{t}^{t+\Delta t} P_{\text{Cooling}}\,dt + \int_{t}^{t+\Delta t} P_{\text{Other Losses}}\,dt \quad (7)\end{aligned}$$

2.2. Efficiency factors of energy conversion

Because it is almost impossible to model the detailed mechanisms of heat transfer from the three sources electric arc, oxidation reactions and gas burners to the melt and slag for the highly unsteady EAF operation due to transport and reaction kinetics of oxidation reactions in melt, slag, and gas phase, due to the erratic behaviour of the electric arcs, and due to the complex heat transfer in the melting scrap pile, we preferred to introduce efficiency values of the energy conversions. E.g., for the energy conversion of electrical energy from the transformers to the steel melt, the efficiencies of the energy transfer to the high current system, η_{el}, and the energy transfer from the electric arcs to the melt, η_{arc}, is considered (Eq.(8)):

$$\Delta H_{\text{Melt, el}} = \eta_{\text{el}}\eta_{\text{arc}} \int_{t}^{t+\Delta t} P_{\text{Electric}}\,dt \quad (8)$$

Typical efficiency of electrical energy transfer to the high current system of an EAF is between η_{el} = electric arc power/(electric arc power + ohmic losses) = 0.88–0.92 [34]. High values apply for modern EAF technology. The efficiency of energy conversion from the electric arc depends on the foaming slag operation that shields the electric arc radiation. Depending on the height of foaming slag the efficiency was found in EAF trials to be in the range η_{el} = electric arc power to the melt/electric arc power = 0.36–0.93 [2]. Highest efficiency values are achieved for long electric arcs that are surrounded by the scrap pile during the boring period (η_{el} = 0.88–0.92) and by short electric arcs that are covered by foaming slag during the late refining period [2]. The combined efficiency of $\eta_{\text{el}}\eta_{\text{arc}}$ of energy conversion from the transformer to the melt is between $\eta_{\text{el}}\eta_{\text{arc}}$ = 0.60–0.80 [18].

The enthalpy portion that is transferred to the melt and slag from the released chemical energy of oxidation reactions in the melt and slag is:

$$\Delta H_{\text{Melt, chem}} = \eta_{\text{chem}} \int_{t}^{t+\Delta t} \sum_i \dot{m}_{\text{Oxidized,i}} h_{\text{Oxidized,i}}\,dt \quad (9)$$

The efficiency factor of energy conversion from chemical energy of oxidation reactions to the steel melt is η_{chem} = 0.70–0.80 [1]. Of special interest is the oxidation of carbon in the steel melt by oxygen injection, because only CO is stable in liquid Fe melt (see Table 3). However, CO gas from the steel melt is oxidized partly to CO_2 in the furnace gas atmosphere with oxygen from infiltrated air or from injected oxygen for CO post-combustion. Off-gas measurements indicate for a large variety of EAFs always a certain amount of $CO + ½O_2 \rightarrow CO_2$ post-combustion due to air infiltration [18–20]. Measured CO_2 concentrations vary between 0 and 25 vol. % at the EAF elbow and corresponding measured CO_2/CO ratio is approximately 0.2–0.4 [18–20]. The energy release from $CO + ½O_2 \rightarrow CO_2$ post-combustion is significant with 7.01 kWh/$m^3_{O_2}$ compared to 2.73 kWh/$m^3_{O_2}$ for $C + ½O_2 \rightarrow CO$ in steel melt (Table 3). Therefore we consider a certain portion of CO post-combustion to the chemical energy contribution in the EAF with an additional efficiency factor for CO post-combustion, η_{PC} = 0.10, as a part of the energy released from CO post-combustion contributes to the EAF heat.

The enthalpy portion that is transferred to the melt and slag from the chemical energy of burner gas combustion is:

$$\Delta H_{\text{Melt, Burners}} = \eta_{\text{Burners}} \int_{t}^{t+\Delta t} P_{\text{NG Burners}}\,dt \quad (10)$$

The efficiency factor of burner energy conversion depends on the heat transfer from the burner flame to the scrap pile. Initially high values of the heat transfer to the cold scrap pile decrease from η_{NG} = 0.70 to η_{NG} = 0.20 at the end of the heat due to molten steel bath covered with slag, Fig. 5 [17]. Due to that significant decrease the EAF burners are applied during the first 5–10 min of melting. A mean value of η_{NG} = 0.50–0.60 is therefore applied to the gas burners.

These three enthalpy portions contribute to the melting and superheating of the melt in the EAF, Eq. (8) to Eq. (10), $\Delta H_{\text{Melt}} = \Delta H_{\text{Melt,el}} + \Delta H_{\text{Melt,chem}} + \Delta H_{\text{Melt,Burners}}$. Using efficiency factors of the energy conversion in the EAF, the energy conservation equation of the EAF process, Eq. (5), is converted to Eq. (11):

$$\begin{aligned}\Delta H_{\text{Melt}} &= \eta_{\text{el}}\eta_{\text{arc}} \int_{t}^{t+\Delta t} P_{\text{Electric}}\,dt + \eta_{\text{chem}} \int_{t}^{t+\Delta t} \\ &\quad \times \sum_i \dot{m}_{\text{Oxidized,i}} h_{\text{Oxidized,i}}\,dt + \eta_{\text{Burners}} \int_{t}^{t+\Delta t} P_{\text{NG Burners}}\,dt \\ &= \int_{T(t)}^{T(t+\Delta t)} h_{\text{Steel}} m_{\text{Steel}}\,dt + \int_{T(t)}^{T(t+\Delta t)} h_{\text{Slag}} m_{\text{Slag}}\,dt \quad (11)\end{aligned}$$

The heat losses to the off-gas system and to the furnace cooling system are considered by the efficiency values of input energy conversion $\eta < 1$.

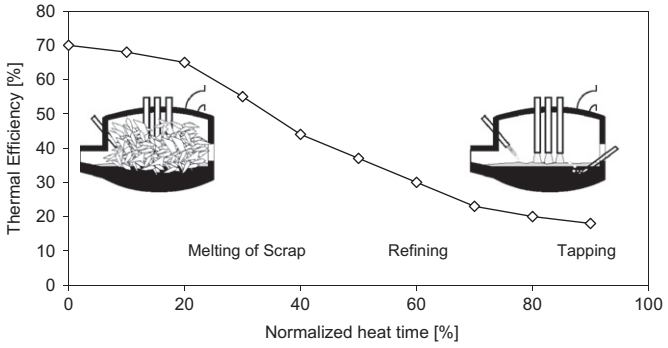

Fig. 5. Efficiency of energy transfer from the burner flame to the steel scrap and melt [17].

2.3. Mass balances

To determine the steel temperature as function of melting time, the masses of oxidized elements in the steel melt during injection of oxygen and the steel mass and slag mass must be determined for each time step. This is provided by solving the total mass balance of the EAF, Eq. (8), and the mass balances of the most important alloy elements i = Fe, C, Si, Al, Mn, Cr, Mo, V, and the slag forming elements CaO, MgO, SiO_2, Al_2O_3, FeO, MnO, Cr_2O_3, Eq. (12):

$$x_{i,Scrap1}\cdot m_{Scrap1} + x_{i,Scrap2}\cdot m_{Scrap2} + \ldots + x_{i,Alloy}\cdot m_{Alloy} + x_{i,Lime}\cdot m_{Lime} + x_{i,Dololime}\cdot m_{DoloLime} + x_{i,Coal}\cdot m_{Coal} = x_{i,Melt}\cdot m_{Melt} + x_{i,Slag}\cdot m_{Slag} + x_{i,Dust}\cdot m_{Dust} \quad (12)$$

For carbon, the following mass balance applies, Eq. (13):

$$x_{C,Scrap1}\cdot m_{Scrap1} + x_{C,Scrap2}\cdot m_{Scrap2} + \ldots + x_{C,Alloy}\cdot m_{Alloy} + x_{C,Lime}\cdot m_{Lime} + x_{C,DoloLime}\cdot m_{DoloLime} + x_{C,Coal}\cdot m_{Coal} = x_{C,Melt}\cdot m_{Melt} + x_{C,Off-gas}\cdot m_{Off-gas} \quad (13)$$

Some oxidation reactions in the steel melt have to be considered in the mass balance equations, e.g. Al + $3/4O_2$ → $½Al_2O_3$, Si + O_2 → SiO_2, C + $½O_2$ → CO, Fe + $½O_2$ → FeO, etc. Oxidation products increase the total mass of slag. The amount of oxidized elements depends mainly on the amount of injected oxygen to the melt. However, redox reactions are important for the reduction of FeO with carbon injected to the foaming slag and the reduction reaction due to FeO component in DRI, $FeO_{Slag} + C = Fe_{Melt} + CO$.

Experiences from industrial EAF operation show that injected oxygen is not completely transferred to the reaction with components of the steel melt, but there are oxygen losses from the supersonic oxygen gas jet to the gas phase (turbulence and/or post-combustion reaction with CO) or to the slag phase (e.g. direct reaction with injected carbon fines to generate foaming slag). Usual oxygen losses due to imprecise lance operation are in the order of 20%, i.e. an efficiency of mass conversion of the oxygen lances and injectors $\eta_{O2} = 0.80$.

Having determined the masses of steel and slag and the enthalpy transferred to the steel malt and slag, the steel temperature is determined from temperature integration over standard heat capacity of the steel. Typical specific slag masses of the EAF process are in the range from 70 kg/t to 150 kg/t.

3. Characteristics of direct reduced iron input to EAF operation

A brief comparison between the typical operation parameters of some scrap and DRI-based EAFs are given in Table 4 with mean values of 16 industrial EAFs. The substitution of steel scrap with DRI increases the time needed for melting the EAF charge (Power-on time). This is attributed to the lower melting rate of DRI caused by the FeO that needs to be reduced. Moreover, having an acidic slag caused by the SiO_2-, Al_2O_3-containing gangue materials in the DRI, it is also obvious that the specific consumption of lime and dolomite increases to manage the appropriate slag basicity near $x_{CaO}/x_{SiO2} = 2$. Due to the higher slag masses in the DRI-based EAF, one need again longer melting time to bring the slag into solution and accordingly need more electrical energy consumption with respect to the scrap-based EAFs.

The oxygen consumption is similar in both cases. The lower oxygen consumption of the DRI-based EAF is explained with the higher iron oxide input with DRI. While in the case of total carbon used (injected as carbon fines and added as lump coke), the amount of carbon in the selected DRI furnaces is relatively high with respect to the amount of oxygen injected. The additional carbon also supplied through the DRI partially supports the combustion process, i.e. the chemical energy input. Finally, a great difference between natural gas consumption in both furnaces is also obvious. This is attributed to the need of natural gas mainly during melting/boring of steel scrap, where the heat transfer efficiency from the hot gas atmosphere to the rather cold scrap is high (Fig. 5). Having small portion of scrap in the DRI-EAFs and operating on flat mode basis for melting continuously charged DRI does not then necessitate natural gas injection. In that sense, it should be noted that operating on flat mode basis most the heat during DRI usage also increase the potential of the arc radiation to the refractory side walls and accordingly decreases the average lifetimes of the furnace campaigns. To optimize the lifetime of the campaign, a strict monitoring of the slag foaminess and its management is then important.

Table 4
EAF operation parameters for scrap-based versus DRI-based charges.

	Scrap based*	DRI based**
Power-on time, min	39	57
Tap-to-Tap time, min	52	68
Lime, kg/t_{steel}	29	46
Dolomite, kg/t_{steel}	5	14
Carbon, kg/t_{steel}	17	23
Oxygen, m^3/t_{steel}	32	28
Natural gas, m^3/t_{steel}	5	0–1.5
Energy consumption, kWh/t_{steel}	391	570

*: Average of 8 AC-EAFs, **: Average of 5 AC-EAFs with approx. 80% DRI, Metallization: 92.5%, C%: 2%; Most furnaces of average performances.

According to the endothermic reduction reaction of FeO by carbon, FeO + C = Fe + CO, and the more slag volume encountered by DRI usage, the electrical energy demand of the EAF generally increases with increasing share of DRI as metallic charge (Fig. 6). However, in very rare cases the substitution of scrap raw material of very low quality, i.e. with a high portion of non-ferrous gangue materials, with DRI can result in a decreasing specific energy demand when parts of the scrap are substituted with DRI of relatively higher quality. Both trends are shown from observed EAF production data in Fig. 6. Generally speaking, the electrical energy demand increases more or less linearly with the share of DRI in the EAF.

Koehle provided an EAF process model based on multiple linear regression of a large database of available EAF process data [22,23]. The objective was to establish a relation between well-known EAF process parameters as specific scrap input, specific weight of slag formers, oxygen consumption, tap temperature, etc., and the

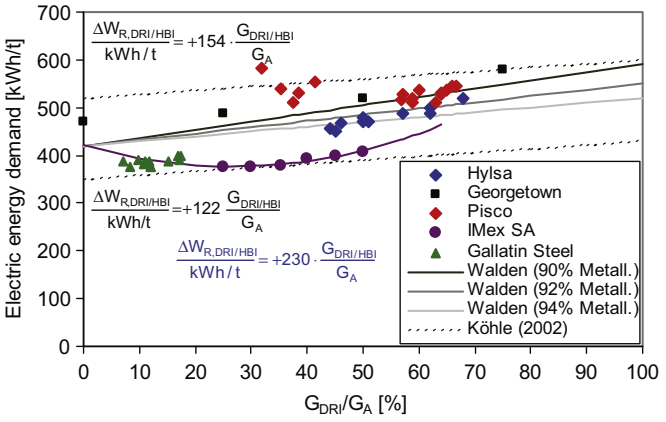

Fig. 6. Electrical energy demand of the EAF as function of specific mass input of direct reduced iron for various steel plants [7,18,27,32,37,45].

electrical energy demand of the EAF. One of the linear model parameters was the specific amount of DRI input mass, G_{DRI}/G_A, where G_A denotes the weight of tapped steel. The Koehle model indicated a positive correlation coefficient between specific amount of direct reduced iron and electrical energy demand of the EAF (Eq. (14)) which represents a good approximation of the observed EAF operation data in Fig. 6.

$$\frac{\Delta W_{el,DRI}}{kWh/t} = +80\frac{G_{DRI}}{G_A} \quad (14)$$

In very analogous manner to the Koehle approach [22,23], Adams et al. proposed a linear model to determine the total energy demand of the EAF process [1]. He applied a negative correlation coefficient between DRI input, G_{DRI}/G_E, where G_E denotes the weight of all ferrous input, and the total energy, Eq. (15), also indicated in Fig. 6.

$$\frac{\Delta W_{total,DRI}}{kWh/t} = -100\frac{G_{DRI}}{G_E} \quad (15)$$

Walden [42] provided a positive correlation between electrical energy demand and DRI input (indicated in Fig. 6) considering the metallization degree of DRI, M_{DRI} in %:

$$\frac{\Delta W_{el,DRI}}{kWh/t} = 100 + 17.5 \times (94 - M_{DRI})\frac{G_{DRI}}{G_A} \quad (16)$$

Following the linear regression approach from Koehle [22], Conejo and co-worker [9,10] developed a model of the electrical energy demand of 100% DRI charges in the EAF. Model coefficients were derived by assessment of 1122 DRI heats of a steel plant in Mexico. Additional terms in the regression model consider metallization degree, M_{DRI}, carbon content of DRI in %, C_{DRI}, and gangue content of DRI in %, G_{DRI} (Eq. (17)):

$$\frac{\Delta W_{el,DRI}}{kWh/t} = 384.365\frac{G_{DRI}}{G_A} - 0.391\,M_{DRI} - 17.849\,C_{DRI} + 4.296\,G_{DRI} \quad (17)$$

However, as the model was calibrated at 100% DRI heats of one steel plant the application of the Conejo DRI model to EAF heats of scrap and DRI mixtures is limited. Mixtures of scrap and DRI input in the EAF are economic and most common (see Table 5 and [15]).

A positive correlation between electrical energy demand and DRI portion is proved by operation data from three EAF steel plants, Hylsa, +230 kWh/t · G_{DRI}/G_A, Georgetown, +154 kWh/t · G_{DRI}/G_A, and Gallatin Steel, +122 kWh/t · G_{DRI}/G_A [7,15,45]. However, EAF operation data from Pisco steel plant indicate decreasing electrical energy demand with increasing DRI share in agreement with the Adams model. Hornby-Anderson [16] reported increasing electrical energy demand. However, the specific electrical energy data of the DRI/scrap mixes are lower than the 100% scrap reference heat (Fig. 6, [16]). Conejo [10] determined a clearly positive correlation coefficient between electrical energy demand and DRI content to +132 kWh/t · G_{DRI}/G_A. We estimated the range of correlation coefficients between the share of DRI to the total ferrous input mass to the electrical energy demand from mass and energy balances to −70–+80 in Eq. (14) [34]. The range from negative to positive correlation coefficients indicates that the detailed characterization and classification of the input materials, e.g. heavy scrap, light scrap, chips, etc. is evident for a precise determination of the electrical energy demand. Occasionally the input temperature of hot charged DRI has to be considered for the EAF energy balance, e.g. for the Fasteel process [39,40]. However, most EAF plants report increasing electrical energy demand with increasing input of DRI indicating a high potential for process optimization.

Table 5
Mean process parameters of investigated heats of 16 EAFs charged with 100% steel scrap to 94% DRI (cold charged).

EAF no.	DRI [%]	Scrap [%]	Electrical energy [kWh/t]	Oxygen [m^3/t]	NG [m^3/t]
1	90	10	600	28	0.0
2	94	6	590	22	0.0
3	80	20	640	5	0.0
4	80	20	470	23	1.6
5	70	30	600	5.5	0.0
6	0	100	420	40	3.3
7	0	100	450	33	4.8
8	0	100	370	27	5.9
9	0	100	440	24	0.0
10	0	100	310	40	4.3
11[a]	0	100	500	8.7	0.0
12[a]	0	100	500	8.7	1.2
13[a]	0	100	520	10	0.0
14	0	100	400	32	0.0
15	0	100	460	38	5.0
16	0	100	390	36	8.0

[a] High alloyed stainless steel.

4. Model results

The mass and energy model as described in chapter 2 was used to model the expected energy demand of EAF processes charged either with 100% steel scrap or with mixes of steel scrap and DRI. We present exemplary results from 4 case studies about the expected electrical energy demand:

- Increase of DRI to scrap ratio in an 80 t EAF
- Use of lime instead of limestone in EAF for stainless steel production
- Increase of tap weight of a 160 t EAF
- Increase of oxygen consumption in 90 t EAF

4.1. Increase of DRI to scrap ratio in an 80 t EAF

The mean electrical energy demand of 80 t EAF applying 90% DRI and 10% steel scrap was about 580 kWh/t, mean oxygen consumption was about 32 $m^3_{O_2}$/t, mean tapping temperature 1660 °C. There is no gas burner installed. Carbon concentration of DRI was 2%, 93% metallization degree, 1% CaO, 1.4% SiO_2, 8.3% FeO gangue material. 50 kg/t lime and 7 kg/t dolomitic lime was charged as slag formers. 14 kg/t carbon fines was injected for FeO reduction and foaming slag generation. Applying the following efficiency values from Eq. (11) in the energy model, $\eta_{el}\eta_{arc} = 0.70$, $\eta_{chem} = 0.75$, $\eta_{NG} = 0.55$, $\eta_{PC} = 0.10$, the reported process parameters of the 80 t EAF were reproduced in detail. The calculated metal yield of 87.5% agrees well with the observed value. The specific slag mass was calculated to 119 kg/t. The chemical energy input of the EAF was determined to 311 kWh/t. This value represents the total of the exothermic oxidation reaction from application of 32 m^3/t oxygen and the endothermic reduction reaction of FeO in the slag and in DRI. The total energy demand is determined to 893 kWh/t. This value corresponds well to the documented range of complete EAF energy balances [18]. A decrease of electrical energy demand was expected by increasing the chemical energy.

Model results with varying oxygen capacity and consumption are given in Fig. 7 indicating the expected electrical energy saving with increasing oxygen consumption to −5.4 $kWh_{el}/m^3_{O_2}$. Also shown are the predictions of the Koehle regression model indicating a lower electrical energy level of the particular EAF process and a lower expected electrical energy saving per m^3/t additional oxygen, −4.3 $kWh_{el}/m^3_{O_2}$.

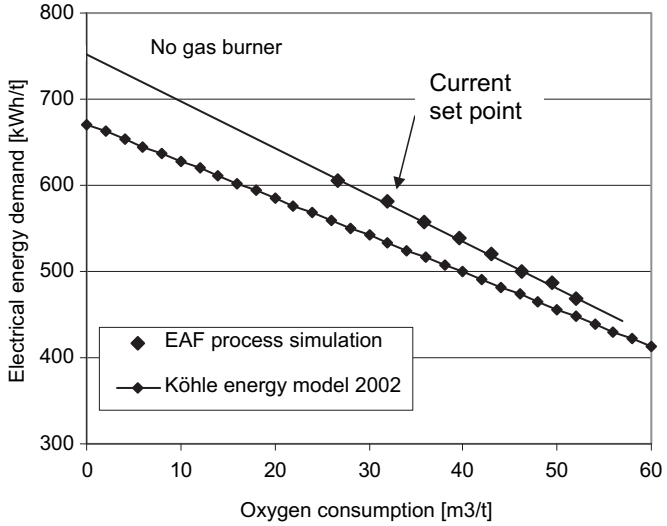

Fig. 7. Calculated relationship between electric energy demand and oxygen consumption of an 80 t EAF for the presented model and for the Koehle model.

The calculated relation between electrical energy demand and burner gas consumption is shown in Fig. 8. The expected energy saving is determined to $-6.7\ kWh_{el}/m^3_{NG}$ for the oxy-fuel burner. The correlation coefficient between natural gas consumption and electrical energy demand of the Koehle model, $-8.0\ kWh_{el}/m^3_{NG}$, is higher.

2 m^3 oxygen are required for the stoichiometric combustion of 1 m^3 natural gas. It is interesting to note that the decrease of electrical energy in kWh per m^3 oxygen is more efficient for direct oxygen injection to the melt ($-5.4\ kWh_{el}/m^3_{O_2}$ and $-4.3\ kWh_{el}/m^3_{O_2}$) and less efficient for oxy-fuel burners ($-3.3\ kWh_{el}/m^3_{O_2}$ and $-4.0\ kWh_{el}/m^3_{O_2}$). Combustion natural gas in the EAF, however, is in most cases beneficial to total CO_2 emission figures of EAF steelmaking due to its high efficiency of heat transfer to the cold scrap pile [21].

The influence of varying DRI to scrap ratio on the EAF process parameters are shown in Fig. 9. The same tap weight and tapping temperature were objectives of the model calculations. Lime input was modified to maintain the same slag basicity CaO/SiO_2 at tap. The injected amount of oxygen injection was adapted in order to

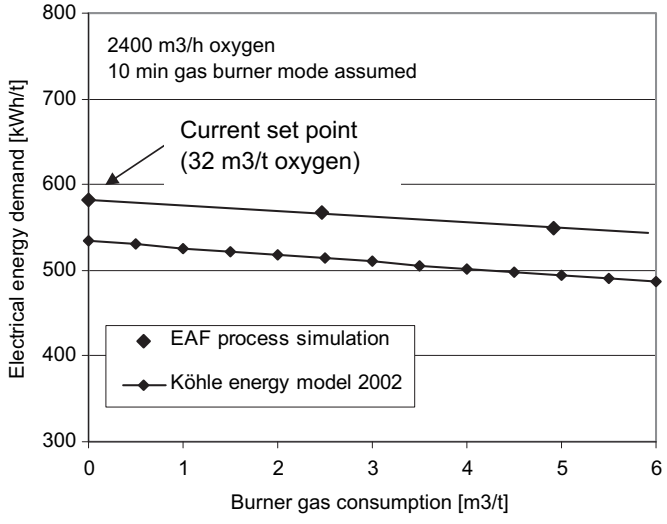

Fig. 8. Calculated relationship between electric energy demand and burner gas consumption of an 80 t EAF for the presented model and for the Koehle model.

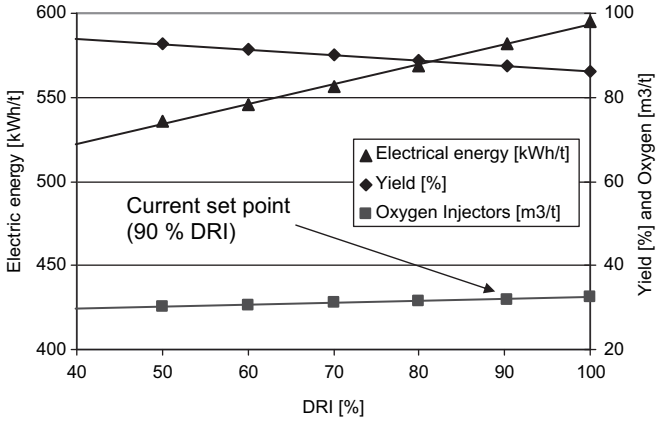

Fig. 9. Calculated influence of varied DRI to steel scrap ratio on EAF process parameters as specific oxygen consumption, metal yield and electrical energy demand (current set-point of the investigated EAF at 90% DRI).

maintain same carbon content at tapping (0.15%) and approximately the same FeO concentration in the slag at tapping.

Model results indicated small changes of electrical energy demand ($+1.19\ kWh_{el}/t$), metal yield (−0.13%), and oxygen consumption ($+0.046\ m^3_{O_2}/t$) for each % DRI increase. The calculated gradient between electrical energy demand and DRI portion, $+119\ kWh_{el}/t\ G_{DRI}/G_A$, corresponds to the positive trend in the Koehle model ($+80\ kWh_{el}/t\ G_{DRI}/G_A$) [22,23] and agrees very well with the Walden model for DRI with a 93% metallization, $117.5\ kWh_{el}/t\ G_{DRI}/G_A$ [42].

The low increase of oxygen consumption indicates the almost balanced input of excess carbon and FeO with DRI in this case, that requires little adaptation by external oxygen. This behaviour depends sensitively on DRI composition. However, the expected increase of electrical energy demand with increased DRI input could be compensated by increase of chemical energy input with slightly increased oxygen consumption.

4.2. Use of lime instead of limestone in EAF for stainless steel production

It is common EAF operation practise to add lime and dolomitic lime as slag formers. However, limestone was used as slag former in EAF for high-alloyed stainless steel production in order to minimize production costs and to provide CO/CO_2 gas from $CaCO_3$ dissociation for bath movement and slag foaming while oxygen consumption was low due to stainless steel production. The electrical energy demand was 500 kWh/t and 8.7 m^3/t oxygen consumption. It was suggested to replace 50 kg/t limestone by lime in order to decrease electrical energy demand and to substitute lime with 15% doloma to decrease wear of magnesia-based side wall lining in the EAF. The calculated decrease of 25 kWh/t electrical energy demand was in agreement with observed savings during campaigns for process improvement.

4.3. Increase of tap weight of a 190 t EAF

After revamping a 190 t EAF, the mean tap weight will be increased from 157 t to 165 t as possible with existing transformer or oxygen injector capacity. Current process data showed 390 kWh/t electrical energy demand, 36 m^3/t oxygen consumption and 8 m^3/t natural gas consumption. From the current process data of the 190 t EAF the total energy demand of 738 kWh/t and 130 kg/t specific slag mass was calculated. Assuming a proportional increase of input materials as steel scrap – with a relatively

high amount of shredder, lime, coal and carbon fines, and considering constant specific consumption of oxygen the model predicted an increase of electrical energy demand to 392 kWh/t. The additional 3500 kWh electrical energy required either an increase of 2 min power-on time or with slightly increasing consumption of oxygen and natural gas and increase of 1 min power-on time. The mean tap-to-tap time remained unchanged. The Koehle model [22] predicted a decrease of electrical energy demand from 279 kWh/t (157 t tapped) to 278 kWh/t (165 t tapped). The discrepancy of the values determined by the Koehle model with observed process data of the 190 t EAF is due to the important influence of shredder to the model results, ΔW_{el}/[kWh/t] = $-50\ G_{Shr}/G_A$ [22,23], indicating an over-estimation of the impact of shredder to the electrical energy demand.

4.4. Increase of oxygen consumption in 90 t DRI-EAF

Current operation data of a 90 t EAF charged with 90% DRI and 10% steel scrap revealed 680 kWh/t electrical energy demand, 5 m^3/t oxygen consumption and 5 kg/t carbon fines injection, 55 kg/t lime consumption. Model parameters are given in Table 6. For a suggested installation of advanced oxygen technology with an increase of oxygen consumption to 25 m^3/t and an increase of injected carbon fines to 10 kg/t the model predicted a 68 kWh/t decrease of the electrical energy demand. The corresponding correlation coefficient between electrical energy demand and oxygen consumption, $-2.7\ kWh_{el}/m^3_{O_2}$, is lower in this case than in most EAF process models, e.g. $-4.0\ kWh_{el}/m^3_{O_2}$ in the Koehle model [22,23]. However, this is explained with the relatively low efficiency of oxygen injection due to high amounts of FeO from medium quality DRI that is continuously fed to the EAF. Thus, increase of metallization degree of DRI is more promising in order to decrease the high electrical energy demand. The expected operation parameters of the 90 t EAF with 90% DRI and 25 m^3/t oxygen consumption, 610 kWh/t electrical energy demand is in good agreement with other process data of DRI-EAFs in Table 5.

The presented model was applied to 16 EAFs in steel industry charged with 100% steel scrap to 94% DRI (Table 5). The calculated electrical energy demand using the set of mean efficiency values of the energy conversions, $\eta_{el}\eta_{arc} = 0.70$, $\eta_{chem} = 0.75$, $\eta_{NG} = 0.55$, $\eta_{PC} = 0.10$, is shown versus the observed electrical energy demand in Fig. 10. The overall acceptable agreement indicate, that the model based on simple mass and energy balances provides a reasonable first order approximation of the energy balance of the EAF charged

Table 6
Adapted efficiency values of oxygen and energy conversion for 16 EAFs charged with 100% steel scrap to 94% DRI in order to precisely reproduce the observed process parameters.

	η_{O2} [%]	$\eta_{el}\eta_{arc}$ [%]	η_{chem} [%]	η_{NG} [%]	η_{PC} [%]
Range from various studies [11]	80–90	60–80	70–80	50–60	10–40
EAF no. 1, 90% DRI	83	65	74	55	10
EAF no. 2, 94% DRI	84	66	74	55	10
EAF no. 3, 80% DRI	82	66	73	55	10
EAF no. 4, 80% DRI	90	68	75	55	10
EAF no. 5, 70% DRI	83	65	74	55	10
EAF no. 6, 100% scrap	84	69	74	55	10
EAF no. 7, 100% scrap	85	68	74	55	10
EAF no. 8, 100% scrap	86	68	74	55	10
EAF no. 9, 100% scrap	80	70	75	55	10
EAF no. 10, 100% scrap	90	68	75	55	10
EAF no. 11, 100% scrap[a]	83	74	74	55	10
EAF no. 12, 100% scrap[a]	84	68	74	55	10
EAF no. 13, 100% scrap[a]	82	67	73	55	10
EAF no. 14, 100% scrap	90	80	75	55	10
EAF no. 15, 100% scrap	90	67	75	55	10
EAF no. 16, 100% scrap	76	67	70	55	10

[a] High alloyed stainless steel.

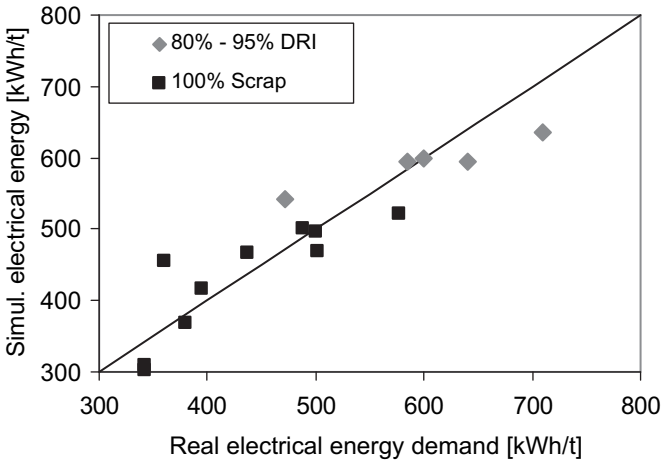

Fig. 10. Calculated electric energy demand versus observed electric energy demand for fixed model parameters (efficiency values of energy conversion ($\eta_{el}\eta_{arc} = 0.70$, $\eta_{chem} = 0.75$, $\eta_{NG} = 0.55$, $\eta_{PC} = 0.10$).

with steel scrap or with DRI or mixtures. However, the efficiency values of energy transfer from the electric arcs, from the oxidation reactions, from the gas burners to the melt were adapted for each EAF in order to reproduce the EAF operation set-points with higher precision (Fig. 11). As a result, the efficiency values were not fixed to the initial values ($\eta_{el}\eta_{arc} = 0.70$, $\eta_{chem} = 0.75$, $\eta_{NG} = 0.55$, $\eta_{PC} = 0.10$) but varied in ranges that were derived in independent studies on energy transfer in the EAF [2,17,18,34], i.e. $0.6 < \eta_{el}\eta_{arc} < 0.8$, $0.7 < \eta_{chem} < 0.8$, $0.5 < \eta_{NG} < 0.6$, $0.1 < \eta_{PC} = 0.4$ (Table 6). The variation of efficiency values is not surprising as the installed EAF technology, transformers and oxygen injector technology may significantly vary from furnace to furnace resulting in different efficiencies of energy and mass conversion. E.g., the arc operation at a high power factor in the range near 0.8 results in a long free arc length and provides the energy transfer to the surrounding scrap with high efficiency. However, the EAF operation at high power factors requires efficient shielding of the burning electric arcs with foaming slag when the scrap pile is melted down. Foaming slag operation depends on slag chemical composition and, more important, controlled injection of oxygen and carbon fines to the slag in order to provide sufficient gas volume and appropriate slag viscosity at a defined FeO content. Careful foamy slag operation and control is therefore crucial for a high-energy conversion efficiency of electrical energy, η_{arc}.

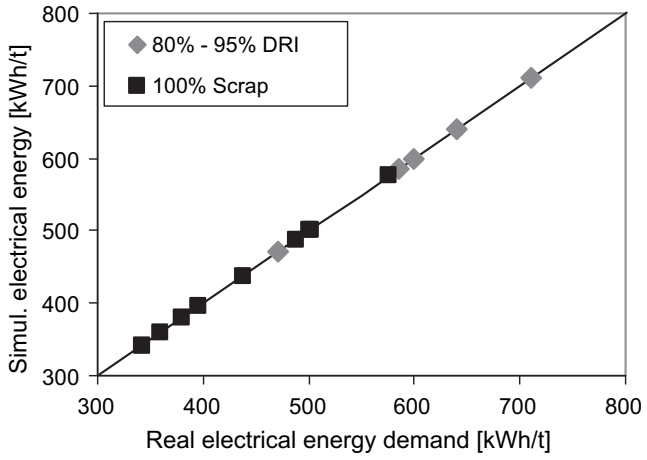

Fig. 11. Calculated electric energy demand versus observed electric energy demand for adapted model parameters (i.e. efficiency values of energy conversion in Table 6).

5. Conclusion

A model of the EAF energy efficiency was developed based on closed mass and energy balance of the EAF melting process. Input parameters comprise EAF processes based on steel scrap, DRI, HBI and pig iron. This model was applied to industrial EAFs in steel industry charged with 100% scrap or with mixes of scrap and DRI up to 95% DRI. Very complex mass and energy conversion of the EAF melting process was simplified with efficiency factors of heat transfer from the various energy sources as electric arcs, oxidation reactions in the steel melt, combustion reactions and post-combustion of CO gas emitted from the steel melt. These efficiency values are in excellent agreement with ranges from previous independent studies. The model provides additional information on the EAF process, that are hardly measured in industrial steelmaking plants, e.g. chemical energy input and total energy demand or slag mass and enthalpy. Model results were illustrated for case studies about increase of DRI to scrap ratio, changes in input masses, and increase of oxygen consumption. The model is used to determine the total energy demand of the particular EAF process and to predict the expected changes in operating parameters and site-specific operating costs of the EAF process with proposed changes in oxygen technology or slag operation. The extension of the model to EAF process with continuous feeding as continuous scrap pre-heating systems or the input of hot metal is optional.

References

[1] Adams W, Alameddine S, Bowman B, Lugo N, Paege S, Stafford P. Total energy consumption in arc furnaces. MPT International; 2002:44–50.
[2] Ameling D, Sittard M, Ullrich W, Wolf J. Untersuchungen zur Schaumschlackebildung im Elektrolichtbogenofen. Stahl und Eisen 1986;106:625–30.
[3] Ameling D, Endemann G, Igelbüscher A. Carbon dioxide – curse or future?. In: Metec InsteelCon 2011 conference proceedings. Düsseldorf: Steel Institute VDEh; 2011. p. 4.
[4] Bandusch L. The EAF route for production of high quality steel grades based on DRI. In: 8th European electric steelmaking conference proceedings. Birmingham: 2005, 6 pp.
[5] Barati M. Energy intensity and greenhouse gases footprint of metallurgical processes: a continuous steelmaking study. Energy 2010;35:3731–7.
[6] Becerra J, Duarte P. Environmental emissions compliance and reduction of greenhouse gases in a DR-EAF steel plant. In: AISTech 2008 Conference Proceedings. Pittsburgh: American Iron and Steel Society; 2008. p. 10.
[7] Billard R, Resler S. The use of DRI in the electric arc furnace at Georgetown Steel Corporation. In: 5th European Electric Steelmaking Conference Proceedings. Paris: Association Technique de la Siderurgie Francaise; 1995. p. 37–44.
[8] Birat JF, Hanrot F, Danloy G. CO_2 mitigation technologies in the steel industry: a benchmarking study based on process calculations. Stahl und Eisen 2003; 123:69–72.
[9] Cárdenas JG, Conejo AN, Gnechi GG. Optimization of energy consumption in electric arc furnaces operated with 100 % DRI. In: 16th International Metallurgical & Material Conference, Metal 2007 Conference Proceedings. Hradec nad Moravici: 2007, 7 p.
[10] Conejo AN, Cárdenas JG. Energy consumption in the EAF with 100 % DRI. In: AISTech 2006 Conference Proceedings. Cleveland: American Iron and Steel Society; 2006. p. 529–35.
[11] Duarte PE, Tanavo A, Zendejas E. Achieving carbon-free emissions via the Energiron DR process. In: AISTech 2010 Conference Proceedings. Pittsburgh: American Iron and Steel Society; 2010. p. 165–73.
[12] Fruehan R, Fortini O, Praxton H, Brindle R. Theoretical minimum energies to produce steel for selected conditions. Carnegie Mellon University Pittsburgh. Report for U.S. Department of Energy, Office of Industrial Technologies; March 2000.
[13] Höhne N, Moltmann S, Hagemann M, Angelini T, Gardiner A, Heuke R. Factors underpinning future action – country fact sheets. Ecofys; 2008:151.
[14] Hornby-Anderson S. Educated use of DRI/HBI improves EAF energy efficiency and yield and downstream operating results. In: Associatione Italiana di Metallurgia, editor. 7th European Electric Steelmaking Conference Proceedings. Venice: Associatione Italiana di Metallurgia; 2002. p. 26–9.
[15] Hornby-Anderson S, Metius G, McClelland J. Future green steelmaking technologies. In: Iron and Steel Society, editor. 60th Electric Furnace Conference Proceedings. San Antonio: American Iron and Steel Society; 2002. p. 175–91.
[16] Hornby-Anderson S, Trotter D, Varcoe D, Reeves R. Use of DRI and HBI for nitrogen control of steel products. In: 60th Electric Furnace Conference Proceedings. San Antonio: American Iron and Steel Society; 2002. p. 687–702.
[17] Jones J. New steel melting technologies: Part II, oxy-fuel burner application in EAF. Iron and Steelmaker 1996;23:63–5.
[18] Kirschen M. Energieeffizienz und Emissionen der Lichtbogenöfen in der Stahlindustrie [(Energy efficiency and emissions of electric arc furnaces in steel industry)]. Düsseldorf, Germany: Verlag Stahleisen, ISBN 978-3-514-00739-0; 2007.
[19] Kirschen M, Pfeifer H, Wahlers F. Off-gas measurements for mass and energy balances of a stainless steel EAF. In: 59th Electric Furnace Conference Proceedings. Phoenix: American Iron and Steel Society; 2001. p. 737–45.
[20] Kirschen M, Velikorodov V, Pfeifer H, Kühne R, Lenz S, Loh J, et al. Off-gas measurements at the EAF primary dedusting system. In: 8th European Electric Steelmaking Conference Proceedings. Birmingham: 2005, pp. 563–76.
[21] Kirschen M, Risonarta V, Pfeifer H. Energy efficiency and the influence of gas burners to energy related CO_2 emissions of electric arc furnaces in steel industry. Energy 2009;34:1065–72.
[22] Köhle S. Recent improvements in modelling energy consumption of electric arc furnaces. In: Associatione Italiana di Metallurgia, editor. 7th European Electric Steelmaking Conference Proceedings. Venice: Associatione Italiana di Metallurgia; 2002. p. 1.305–14.
[23] Köhle S, Hoffmann J, Baumert J, Picco M, Nyssen P, Fillipini E. Improving the productivity of electric arc furnaces. European Commission Directorate-General for Research, Research Fund for Coal and Steel; 2003 (Final Report EUR20803).
[24] Kopfle JT, Metius GE. Environmental benefits of natural gas direct reduction. In: American Iron and Steel Society, editor. AISTech 2010 conference proceedings. Pittsburgh: American Iron and Steel Society; 2010. p. 193–8.
[25] Kundrat D, Wyatt A., Fuchs H, González R.L., López Acosta F, Ayala S.A. Improvement of energy consumption in ArcelorMittal Lazaro Cardenas EAF under conditions of uncertain DRI quality. In: 8th European Electric Steelmaking Conference Proceedings. Birmingham: 2005, 10 p.
[26] Lee M, Trotter D, Mazzei O. The production of low phosphorus and nitrogen steels in an EAF using HBI. Scandinavian Journal of Metallurgy 2001;30:286–91.
[27] Lockmeyer D, Yalamanchili B. Use of CIRCAL HBI in the EAF steelmaking at North Star steel Texas. In: 59th Electric Furnace Conference Proceedings. Phoenix: American Iron and Steel Society; 2001. p. 587–94.
[28] Lule R, Lopez F, Espinoza J, Torres R, Morales RD. The production of steels applying 100% DRI for nitrogen removal - the experience of ArcelorMittal Lazaro Cardenas flat carbon. In: AISTech 2009 Conference Proceedings. St. Louis: American Iron and Steel Society; 2009. p. 489–98.
[29] Luengen HB, Endemann G, Schmöle P. Measures to reduce CO_2 and other emissions in the steel industry in Germany and Europe. In: AISTech 2011 Conference Proceedings. Indianapolis: American Iron and Steel Society; 2011. p. 1071–82.
[30] Midrex. World direct reduction statistics, www.midrex.com; 2009. 12 pp.
[31] Morales R, Rodriguez-Hernandez H, Conejo A. A mathematical simulator for the EAF steelmaking process using direct reduced iron. ISIJ International 2001;41:426–35.
[32] Mullen J. Batch charging of DRI at Gallatin Steel. Midrex report no.4; 2000.
[33] N.N. Siemens VAI. Finmet presentation Johannesburg, April 2003, Siemens-VAI report.
[34] Pfeifer H, Kirschen M, Simoes JP. Thermodynamic analysis of EAF electrical energy demand. In: 8th European Electric Steelmaking Conference Proceedings. Birmingham: 2005, pp. 211–232.
[35] Price L, Sinton J, Worrell E, Phylipsen D, Huc X, Lid J. Energy use and carbon dioxide emissions from steel production in China. Energy 2002;27:429–46.
[36] Rummler T, Apfel J, Belous J, Doninger T, Knoth V. High productivity with low emissions – challenge for tomorrow. In: AISTech 2008 conference proceedings. Pittsburgh: American Iron and Steel Society; 2008. p. 8.
[37] Schliephake H, Steffen R, Lüngen H. Einsatzstoff Eisenschwamm und Eisenkarbid. In: Heinen K, editor. Elektrostahlerzeugung. Düsseldorf: Verlag Stahleisen; 1997. p. 65–76.
[38] Scholz R, Pluschkell W, Spitzer K, Steffen R. Steigerung der Stoff- und Energieeffizienz sowie Minderung von CO_2-Emissionen in der Stahlindustrie. Chemie Ingenieur Technik 2004;76:1318.
[39] Simmons J, Manenti A, Shoop K. Consteel to Fasteel: the future of steelmaking. In: American Iron and Steel Society, editor. 60th Electric Furnace Conference Proceedings. San Antonio: American Iron and Steel Society; 2002. p. 377–85.
[40] Simmons J, Shoop K, McCleelland J. Fasteel – the hot metal of Fastmelt and the continuous scrap feeding of Consteel. In: 60th electric furnace conference proceedings. San Antonio: American Iron and Steel Society; 2002. p. 231–40.
[41] Stubbles J. Energy use in the U.S. steel industry: an historical perspective and future opportunities. Columbia: Energetics Inc.; 2000. Report for the U.S. DoE.
[42] Walden K. Metallurgie bei Eisenschwammeinsatz. In: Heinen K, editor. Elektrostahlerzeugung. Düsseldorf: Verlag Stahleisen; 1997. p. 503–11.
[43] World Steel Association. World steel in figures 2011, Brussels, www.worldsteel.org; 2011.
[44] Worrell E, Martin N, Price L. Energy efficiency and CO_2 emissions reduction opportunities in the US iron and steel sector. Energy 2001;26:513–36.
[45] Yanez D, Pedroza M, Ehle J, Knapp H. Shaft furnace technology charging DRI and/or hot metal. In: 6th european electric steelmaking conference proceedings. Düsseldorf: Verein Deutscher Eisenhüttenleute; 1999. p. 24–8.
[46] Zuliani DJ, Scipolo V, Duarte PE, Born C. Increasing productivity and lowering operating costs while reducing GHG emissions in steelmaking. In: Metec InsteelCon 2011 Conference Proceedings. Düsseldorf: Steel Institute VDEh; 2011. p. 10.